Pharmaceutical Research, Vol. 23, No. 7, July 2006 (© 2006)
DOI: 10.1007/s11095-006-0273-y

Research Paper

Comparison of Skin Esterase Activities from Different Species

Jeffery J. Prusakiewicz,[1,2] Chrisita Ackermann,[1] and Richard Voorman[1]

Received October 17, 2005; accepted February 21, 2006

Purpose. Many topically applied drugs contain esters that are hydrolyzed in the skin. Minipigs have emerged as potential models of human dermatology and, in some aspects, may be superior to commonly used rat skin. The aims of this study were to evaluate the suitability of minipig and rat skin as *in vitro* models of human epidermal esterase activity.
Methods. Naphthyl acetate and *para*-nitrophenyl acetate were tested as prototypical substrates of carboxylesterases from skin, plasma, and liver. Reaction products were monitored by high-performance liquid chromatography/ultraviolet analysis.
Results. Hydrolysis efficiency in skin was higher than plasma, but lower than liver. The esterase efficiency of rat skin microsomes (580–1100 min^{-1} mg^{-1}) was two to three orders of magnitude higher than human (1.3–4.2 min^{-1} mg^{-1}) and minipig microsomes (1.2–4.2 min^{-1} mg^{-1}). Rat skin cytosol (80–100 min^{-1} mg^{-1}) was 2- to 10-fold more efficient than human (2.4–67 min^{-1} mg^{-1}) or minipig cytosol (18–61 min^{-1} mg^{-1}). Most importantly, human skin fractions displayed kinetics of hydrolysis very similar to minipig skin.
Conclusions. These studies show minipig skin as an appropriate, potentially valuable model for human epidermal ester metabolism and support the use of minipig skin in preclinical development of topically applied compounds.

KEY WORDS: epidermal drug metabolism; esterase; skin.

INTRODUCTION

Esterases are responsible for hydrolytic biotransformation of endogenous substrates and are critical for various biological processes. Located in the endoplasmic reticulum and cytosol, esterases are widely distributed among tissues and play a major role in drug metabolism and prodrug activation (1). Many esterases display low specificity with regard to xenobiotic substrates. Clinically used drugs containing ester moieties may be susceptible to hydrolysis by esterases (1). Ester-containing prodrugs, such as the anticancer drugs CPT-11 and paclitaxel-2-ethylcarbonate, are activated by hydrolysis (2,3). On the other hand, so-called "soft drugs" contain esters with adjacent moieties that hinder hydrolysis in the skin. Soft drug esters are metabolically stable in skin and might be especially useful for targeting skin with topical delivery and localized exposure. Soft drugs may be readily degraded by plasma esterases after passing through the skin into systemic circulation (1). A better understanding of ester hydrolysis capacity in the skin would increase the utility of ester-containing prodrugs and soft drugs.

Rat skin has been used to study the hydrolysis of topically applied xenobiotic compounds. However, rat skin expresses greater esterase activity than human skin (4). Recent efforts to find an alternative preclinical species have focused on minipigs as a suitable model; given the physiological similarities between minipig and human, this species has emerged as a possible drug metabolism model (5). The permeation characteristics of minipig absorptive mucosa are similar to that of domestic pig and humans, and the minipig liver cytochrome P450 enzymes have properties similar to those of human homologs (5–7). We report here the results of a direct comparison of the esterase activity from three species of skin rat, minipig, and human. *para*-Nitrophenyl acetate (PNPA) and naphthyl acetate (NAc) were used as prototypical esterase substrates, and enzyme activities in skin were compared to plasma and liver esterase activity. In addition, tissue samples were available from various sources making it possible to evaluate the contribution of skin pigmentation in regards to esterase activity.

[1] Department of Pharmacokinetics, Dynamics and Metabolism, Pfizer Global Research and Development, 2800 Plymouth Rd., Ann Arbor, Michigan 48105, USA.
[2] To whom correspondence should be addressed. (e-mail: Jeff.Prusakiewicz@pfizer.com)

ABBREVIATIONS: BNPP, *bis*-(*para*-nitrophenyl) phosphate; NAc, naphthyl acetate; PMSF, phenylmethylsulfonyl fluoride; PNP, *para*-nitrophenol; PNPA, *para*-nitrophenyl acetate.

MATERIALS AND METHODS

Chemicals

Unless otherwise stated, chemical reagents and chromatographic materials were purchased from Sigma-Aldrich (St. Louis, MO, USA).

Tissue Procurement

Rat, porcine, and human plasma were purchased from Bioreclamation (New York, NY, USA). Pooled male rat (198 donors) and male human (10 donors) liver microsomes and cytosolic fractions were purchased from Xenotech (Lenexa, KS, USA). The dorsal skin from ten male Sprague-Dawley rats (150–250 g) were obtained from the animals postmortem after shaving (Charles Rivers Laboratories, Wilmington, MA, USA). Full thickness back skin from four male Yucatan (dark) and five male Gottingen (light) minipigs were obtained from Pfizer (Kalamazoo, MI, USA) or MPI Research (Mattawan, MI, USA). The minipigs ranged in age from 9 to 21 months old. Gottingen minipig livers were obtained from the same animals that skin was procured. Porcine skin was washed and shaved as needed, then frozen at −80°C for further processing. Light (four donors) and dark (two donors) female human skin specimens from reduction mammoplasty procedures, were obtained from the University of Michigan Section of Plastic and Reconstructive Surgery (Ann Arbor, MI, USA).

Preparation of Skin Fractions

The preparation procedures used to generate skin microsomes and cytosol were adapted from standard protocols with slight modification. The skin samples were washed and shaved as needed to remove biological waste that could potentially contain bacterial or fecal esterase activity. Full thickness skin from all species was cleaned of subcutaneous tissue and dermatomed at 350 μm with a Padgett Model S electric dermatome (Integra NeuroSciences, Plainsboro, NJ, USA). Dermatoming epidermal layers of skin aided in the homogenization and prevented contamination by subcutaneous tissue (fat), which contains high levels of esterase activity (8). Dermatomed skin was finely minced and weighed, with 5 mL of KCl/phosphate buffer (150 mM KCl, 100 mM potassium phosphate, pH 7.4) added per gram of tissue. Minced tissues from multiple donors were pooled at this stage to minimize interindividual variability effects. Skin was homogenized on ice using a Brinkmann Polytron. During the homogenization steps, protease inhibitors, which are often included in traditional protocols, were omitted because some of these compounds, such as phenylmethylsulfonyl fluoride (PMSF), are known to inhibit esterases (9). The homogenate was centrifuged at 10,000 × g for 20 min at 4°C to generate the S9 fraction (supernatant). The supernatant was filtered through cheesecloth and centrifuged at 100,000 × g for 1 h at 4°C. The lower speed spin and filtration through cheesecloth helped to remove remaining hair and stratum corneum released during homogenization. The cytosolic fractions were decanted away from the microsomal pellets and saved for further analysis. Because of the weak association of some esterases with membranes, the microsomal enzymes are easily solubilized during routine cell fractionation procedures. Therefore, precautions were taken to minimize microsomal enzyme solubilization (i.e., low salt buffers and no detergents). However, it is still possible that the cytosolic fraction may contain microsomal enzymes that were solubilized during preparation. The microsomal pellets were resuspended in buffer and centrifuged at 100,000 × g again as stated above to obtain washed microsomes. Microsomal pellets were resuspended with a Dounce homogenizer in 50 mM K_2HPO_4, pH 7.4, and frozen at −80°C. All protein concentrations were determined using the Pierce BCA kit method.

Esterase Activity Assay

Incubations (100 μL) containing skin cytosol or microsomes were prewarmed to 37°C for 3 min in 50 mM potassium phosphate, pH 7.4. Reactions were started by the addition of PNPA at eight concentrations ranging from 15 to 2000 μM. After mixing by vortex, samples were allowed to incubate for 10 min at 37°C. The reactions were terminated with 100 μL of cold acetonitrile containing 0.2% formic acid and 100 μM coumarin (internal standard) and placed on ice before centrifugation at 14,000 × g for 5 min at 4°C. Supernatants were transferred to a 96-well microtiter plate, and the plate covered with Costar Thermowell polyethylene sealers and loaded into an autosampler cooled to 10°C. Hydrolysis experiments with NAc at seven concentrations ranging from 15 to 1000 μM were conducted similarly as described above. The enzymatic hydrolysis of PNPA and NAc was first tested for time (0–30 min) and protein linearity, with approximately 10% substrate conversion. All protein concentrations at the reaction time selected (10 min) conformed to pseudo first-order conditions for esterase activity.

Esterase Inhibition Assay

Inhibitions of NAc hydrolysis by PMSF, *bis*-(*para*-nitrophenyl) phosphate (BNPP), and neostigmine were conducted

Table I. PNPA Hydrolysis in Skin Fractions

Enzyme source	K_m (μM)	V_{max} (nmol min^{-1} mg^{-1})	V_{max}/K_m (min^{-1} mg^{-1})
Rat skin microsomes	19 ± 5[a]	2100 ± 100	1100
Light minipig skin microsomes	450 ± 90	55 ± 4	1.2
Dark minipig skin microsomes	260 ± 130	36 ± 7	1.4
Light human skin microsomes	240 ± 40	99 ± 6	4.1
Dark human skin microsomes	660 ± 50	84 ± 3	1.3
Rat skin cytosol	49 ± 12	380 ± 20	80
Light minipig skin cytosol	92 ± 11	170 ± 6	18
Dark minipig skin cytosol	77 ± 26	140 ± 30	18
Light human skin cytosol	78 ± 8	52 ± 2	6.7
Dark human skin cytosol	500 ± 64	120 ± 6	2.4

PNPA: *para*-nitrophenyl acetate.
[a] Data are shown as mean ± standard error and are derived from nonlinear regression analysis of kinetic data from at least three independent determinations and calculated with Graphpad Prism software as outlined in Materials and Methods.

Table II. NAc Hydrolysis in Skin Fractions

Enzyme source	K_m (μM)	V_{max} (nmol min^{-1} mg^{-1})	V_{max}/K_m (min^{-1} mg^{-1})	K_i (μM)
Rat skin microsomes	26 ± 4[a]	1500 ± 70	580	–
Light minipig skin microsomes	85 ± 23	35 ± 3	4.2	–
Dark minipig skin microsomes	77 ± 23	22 ± 2	2.9	–
Light human skin microsomes	260 ± 50	81 ± 6	3.1	–
Dark human skin microsomes	240 ± 40	98 ± 6	4.1	–
Rat skin cytosol	27 ± 4	280 ± 11	100	–
Light minipig skin cytosol	17 ± 3	110 ± 10	61	770 ± 150[b]
Dark minipig skin cytosol	20 ± 5	60 ± 7	29	590 ± 230
Light human skin cytosol	69 ± 8	43 ± 1	62	–
Dark human skin cytosol	78 ± 8	52 ± 2	67	–

NAc: naphthyl acetate.
[a] Data are shown as mean ± standard error and are derived from nonlinear regression analysis of kinetic data from at least three independent determinations and calculated with Graphpad Prism software as outlined in Materials and Methods.
[b] When substrate-dependent inhibition was observed, inhibition constants were calculated by nonlinear analysis of data using Graphpad Prism as outlined in Materials and Methods.

under similar conditions as outlined above, but with slight modifications. These inhibitors were used at or above concentrations that have been found to completely block the enzymatic activity of their respective targets (10–12). Neostigmine (1 μM), BNPP (1 mM), PMSF (1 mM), or the appropriate vehicle was preincubated with various skin fractions at 37°C for 15 min. The hydrolysis reactions were initiated by the addition of NAc (100 μM) as substrate. The reaction was allowed to proceed for 15 min at 37°C followed by the addition of an equal volume of cold acetonitrile containing 0.2% formic acid and 100 μM coumarin (internal standard). Terminated reactions were centrifuged at 14,000 × g for 5 min at 4°C before being transferred to deep-well plates and stored in the autosampler at 10°C.

Product Formation

The formation of products was monitored by high-performance liquid chromatography with photodiode array detection (Shimadzu Corporation, Kyoto, Japan). Peak areas were calculated with the spectrum max mode of the detector. The solvent system consisted of A = 0.1% formic acid containing 3% acetonitrile and B = 0.1% formic acid in acetonitrile. Substrates, products, and standards were chromatographically separated on a Phenomenex Hydro-RP (150 × 4.6 mm, 4 μm) C18 column, at a flow rate of 1 mL/min. The formation of *para*-nitrophenol (PNP) from PNPA was analyzed with a narrow gradient of 55–58% B over 5 min. The formation of naphthol from NAc was analyzed using a gradient ramped from 65 to 100% B over 5 min.

Data Analysis

Product peak areas were recorded and normalized to the coumarin peak area, followed by subtraction of nonenzymatic background. The concentrations of product were calculated by comparison to standard curves of PNP or naphthol. Nonlinear regression analysis was performed with Prism (GraphPad Software, San Diego, CA, USA) using classical Michaelis–Menten equation for all experiments, except for those in which substrate inhibition was observed, in which case a model of substrate inhibition was used.

RESULTS

Kinetics of Skin Esterase Activity

Both PNPA and NAc were metabolized by subcellular skin fractions of all species. Enzymatic reactions were corrected for significant background hydrolysis rates of PNPA in controls. Little if any nonenzymatic hydrolysis was seen in the control samples with NAc. Rat skin fractions were generally higher in activity than minipig or human skin fractions (Tables I and II). In rat skin microsomes, PNPA (Table I) was hydrolyzed with a low K_m and high V_{max}, indicating high affinity and high capacity. For minipig and human microsomes, the K_m was high and the V_{max} was low relative to rat, suggesting low affinity and low capacity. Therefore, the efficiency (V_{max}/K_m) in rat skin microsomes was considerably higher, about three orders of magnitude, than minipig and human skin microsomes.

In rat skin cytosol, the efficiency was greater than that of minipig and human, but to a lesser extent than with microsomes. The efficiency of minipig cytosol was about ten times greater than minipig microsomes, whereas human microsomes and cytosol were about equal. The V_{max} values (52–120 nmol min^{-1} mg^{-1}) observed for PNPA hydrolysis in human skin cytosol agreed with specific activities (80–100 nmol min^{-1} mg^{-1}) previously reported (13). No difference was observed between light and dark minipig skin. However, some differences were observed in human, in that dark skin microsomes and cytosol both displayed higher K_m values than light, translating into lower efficiencies.

For the substrate NAc (Table II), rat skin microsomes again had the highest rate (V_{max}) of hydrolysis and the highest efficiency (V_{max}/K_m) of any skin sample tested. Minipig and human cytosol once again had higher efficiencies than found in their respective microsomes. No significant difference was observed between light and dark skin for either minipig or human. An interesting occurrence was the observation of substrate inhibition by NAc in minipig skin cytosol from both light and dark skin (Fig. 1B and D). In general, human skin displayed kinetic properties of PNPA and NAc hydrolysis that were closer in value to minipig skin than to rat skin.

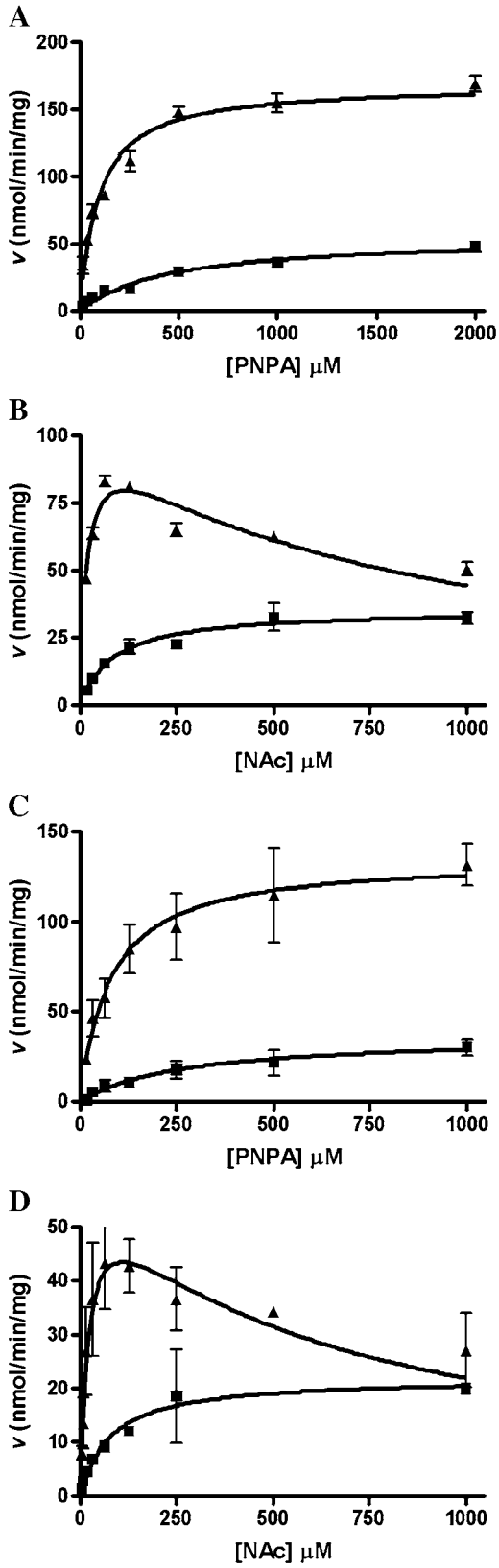

Table III. PNPA Hydrolysis in Plasma

Enzyme source	K_m (μM)	V_{max} (nmol min^{-1} mg^{-1})	V_{max}/K_m (min^{-1} mg^{-1})
Rat plasma	3100 ± 300[a]	230 ± 10	0.74
Human plasma	1100 ± 100	32 ± 2	0.29
Light minipig plasma	1700 ± 200	27 ± 2	0.16
Dark minipig plasma	780 ± 60	46 ± 2	0.59

[a] Data are shown as mean ± standard error and are derived from nonlinear regression analysis of kinetic data from at least three independent determinations and calculated with Graphpad Prism software as outlined in Materials and Methods.

Kinetics of Plasma Esterase Activity

Rat plasma displayed the highest rates of metabolism with both substrates (Tables III and IV). This observation was expected because rat plasma contains carboxylesterase, whereas human plasma does not (14). K_m values were very high in all species, indicating low affinity for both substrates. Reaction velocities for PNPA hydrolysis by rat plasma samples did not reach a plateau in activity, unlike NAc hydrolysis (Fig. 2). Large amounts of protein (0.2–1 mg/mL) were used during the incubations with substrates. Plasma protein binding may have contributed to the elevated K_m values and the absence of a velocity asymptote. Because of high K_m and low V_{max} values, efficiency was much lower in plasma than in skin. PNPA hydrolysis was similar in human and minipig. However, human plasma metabolized NAc at rates 6- to 10-fold higher than minipig plasma. A difference due to pigmentation was not observed for NAc hydrolysis. In contrast, hydrolysis of PNPA was over 3-fold greater in plasma from dark minipig than from light minipig. As with skin fractions, overall, human plasma was closer to minipig plasma than to rat plasma.

Kinetics of Liver Esterase Activity

Liver microsomal esterases were very active in all species toward both substrates. All three species had similar K_m (low) and V_{max} (very high) values, relatively speaking, and consequently, very high efficiencies (Tables V and VI). Rat and human liver microsomes exhibited an 8-fold increase in V_{max} over the cytosol, whereas minipig liver microsomes showed and increase of 127-fold. These results are in agreement with previous reports that over 80% of the activity from rat and human livers was found in the microsomal fraction, and nearly 7% of the microsomal protein from pig liver

Fig. 1. Kinetic analysis of esterase activity in minipig skin fractions. (A) *para*-Nitrophenyl acetate (PNPA) hydrolysis by light minipig skin microsomes (■) and cytosol (▲). (B) Naphthyl acetate (NAc) hydrolysis by light minipig skin microsomes (■) and cytosol (▲). (C) PNPA hydrolysis by dark minipig skin microsomes (■) and cytosol (▲). (D) NAc hydrolysis by dark minipig skin microsomes (■) and cytosol (▲). The data points and error bars represent the mean and standard error, respectively, and represent three independent experiments performed in triplicate.

Table IV. NAc Hydrolysis in Plasma

Enzyme source	K_m (μM)	V_{max} (nmol min^{-1} mg^{-1})	V_{max}/K_m (min^{-1} mg^{-1})
Rat plasma	110 ± 10[a]	190 ± 10	17
Human plasma	320 ± 30	44 ± 1	1.4
Light minipig plasma	450 ± 70	6.1 ± 0.4	0.14
Dark minipig plasma	290 ± 60	6.2 ± 0.5	0.21

[a] Data are shown as mean ± standard error and are derived from nonlinear regression analysis of kinetic data from at least three independent determinations and calculated with Graphpad Prism software as outlined in Materials and Methods.

consisted of nonspecific carboxylesterases (15,16). The efficiencies of liver microsomal fractions were higher than the liver cytosolic fractions (Tables V and VI). This was in contrast to the situation in human and minipig skin, in which cytosol was more efficient than microsomes (Tables I and II). Liver microsomes from light minipig were the most active for both substrates, followed by rat and then by human. This rank order was similar to that observed with purified carboxylesterases from domestic pig, rat, and human liver microsomes (17). The V_{max} value (5.5 μmol min^{-1} mg^{-1}) determined for PNPA hydrolysis by rat liver microsomes was close to the specific activity determined by Heymann and Mentlein (18) (2.42 μmol min^{-1} mg^{-1}). Although the minipig liver microsomes showed a 4-fold higher V_{max} toward PNPA than rat liver microsomes, rat microsomes have a lower K_m value, resulting in the same catalytic efficiency (Table V). Human liver microsomes displayed K_m values of PNPA metabolism 3-fold higher than rat liver microsomes, which resulted in an almost 5-fold lower efficiency for human liver microsomes. In contrast to microsomes, minipig liver cytosol was an order of magnitude less efficient than either rat or human liver cytosol toward PNPA.

Subcellular fractions from all species displayed similar K_m values (11–28 μM) toward NAc. Therefore, the differences in catalytic efficiencies were driven by maximal velocity values (V_{max}). Minipig liver microsomes were 2- and 5-fold more efficient at hydrolyzing NAc than rat or human liver microsomes, respectively (Table VI). Only modest differences were observed between the liver cytosolic fractions, giving rise to very similar catalytic efficiencies (330–400 min^{-1} mg^{-1}). In summary, human liver subcellular fractions were closer in esterase velocity (V_{max}) and catalytic efficiency (V_{max}/K_m) of PNPA and NAc to rat liver fractions than to minipig liver fractions.

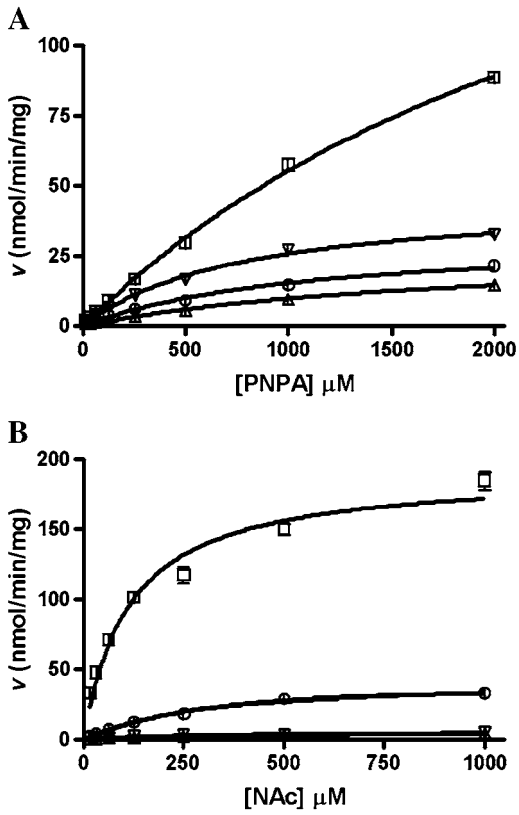

Fig. 2. Kinetic analysis of esterase activity in mammalian plasma. (A) PNPA hydrolysis by plasma from rat (□), light minipig (△), dark minipig (▽), and human (○). (B) NAc hydrolysis by plasma from rat (□), light minipig (△), dark minipig (▽), and human (○). The data points and error bars represent the mean and standard error, respectively, and represent three independent experiments performed in triplicate.

Substrate Dependent Inhibition of Esterase Activity

In studies of NAc hydrolysis, substrate inhibition was observed in both light and dark minipig skin cytosol (Fig. 1B and D). This phenomenon was unique to the skin from minipigs, but was also observed during the metabolism of NAc by all species of liver cytosol and microsomes (Table VI). The K_i observed for NAc in light minipig skin cytosol (770 ± 150 μM) was similar in magnitude to the K_i observed for light minipig liver microsomes (600 ± 230 μM) and cytosol (400 ± 190 μM). Interestingly, the K_i values between liver microsomes and liver cytosol were similar within the same species. Overall, the K_i values for NAc among different species of liver were within 3-fold of each other.

Table V. PNPA Hydrolysis in Liver Fractions

Enzyme source	K_m (μM)	V_{max} (nmol min^{-1} mg^{-1})	V_{max}/K_m (min^{-1} mg^{-1})
Rat liver microsomes	15 ± 5[a]	5500 ± 300	3700
Light minipig liver microsomes	60 ± 9	22,800 ± 800	3800
Human liver microsomes	48 ± 5	3720 ± 90	780
Rat liver cytosol	37 ± 7	660 ± 30	180
Light minipig liver cytosol	96 ± 17	180 ± 10	19
Human liver cytosol	29 ± 9	430 ± 30	150

[a] Data are shown as mean ± standard error and are derived from nonlinear regression analysis of kinetic data from at least three independent determinations and calculated with Graphpad Prism software as outlined in Materials and Methods.

Table VI. NAc Hydrolysis in Liver Fractions

Enzyme source	K_m (μM)	V_{max} (nmol min^{-1} mg^{-1})	V_{max}/K_m (min^{-1} mg^{-1})	K_i (μM)
Rat liver microsomes	24 ± 5[a]	12,500 ± 1000	5300	950 ± 240[b]
Light minipig liver microsomes	17 ± 7	20,700 ± 2900	12,000	600 ± 230
Human liver microsomes	11 ± 2	2700 ± 100	2500	1720 ± 380
Rat liver cytosol	28 ± 4	960 ± 50	340	1470 ± 290
Light minipig liver cytosol	17 ± 10	680 ± 140	400	400 ± 190
Human liver cytosol	15 ± 2	490 ± 18	330	1120 ± 20

[a] Data are shown as mean ± standard error and are derived from nonlinear regression analysis of kinetic data from at least three independent determinations and calculated with Graphpad Prism software as outlined in Materials and Methods.
[b] When substrate-dependent inhibition was observed, inhibition constants were calculated by nonlinear analysis of data using Graphpad Prism as outlined in Materials and Methods.

Hydrolysis Reaction Phenotyping by Esterase Inhibition

Esterase inhibitors were used to differentiate the relative contributions of acetylcholinesterase and carboxylesterases toward the hydrolysis rates of skin fractions. Preincubation with neostigmine, a selective inhibitor of acetylcholinesterase, modestly reduced the hydrolysis rates from all species tested (Fig. 3). Rat skin cytosol was slightly inhibited by neostigmine, whereas rat skin microsomes were not blocked. However, rat skin fractions were completely inhibited by BNPP, a specific carboxylesterase inhibitor. Human and minipig ester hydrolysis activity was reduced by neostigmine, although not by more than 25% (Fig. 3). Interestingly, the amount of activity remaining (18–30%) after pretreatment of human skin fractions with BNPP was very close to the amount of activity inhibited by neostigmine. This relationship between neostigmine and BNPP was also seen with minipig skin microsomes. Light and dark minipig skin cytosolic fractions were inhibited by neostigmine to nearly the same extent (15–25%) as the minipig microsomes. Skin cytosolic fractions from both light and dark minipigs displayed an increased sensitivity to BNPP with less than 5% activity remaining. BNPP and PMSF (a general serine hydrolase inhibitor) displayed very similar results, suggesting that other serine hydrolases do not significantly contribute to NAc hydrolysis in these skin fractions (Fig. 3). Taken together, these results indicate that acetylcholinesterases make minor contributions to ester metabolism, and carboxylesterases are the enzymes responsible for the majority of NAc hydrolysis activity in the skin. Overall minipig skin fractions closely resembled human skin fractions after inhibitor treatment.

DISCUSSION

During prodrug development, ester-containing compounds have been used to increase permeability and modulate pharmacokinetic profiles of existing therapies (4). However, designing tissue-specific activation of ester prodrugs is difficult because of the widespread distribution of esterases throughout the body (19). On the other hand, there is growing evidence that drugs containing esters may be useful for topical application (4). Many skin pathologies, such as melanoma and psoriasis, have therapeutic targets that are directly accessible through topical application. It would be advantageous to design compounds containing metabolically

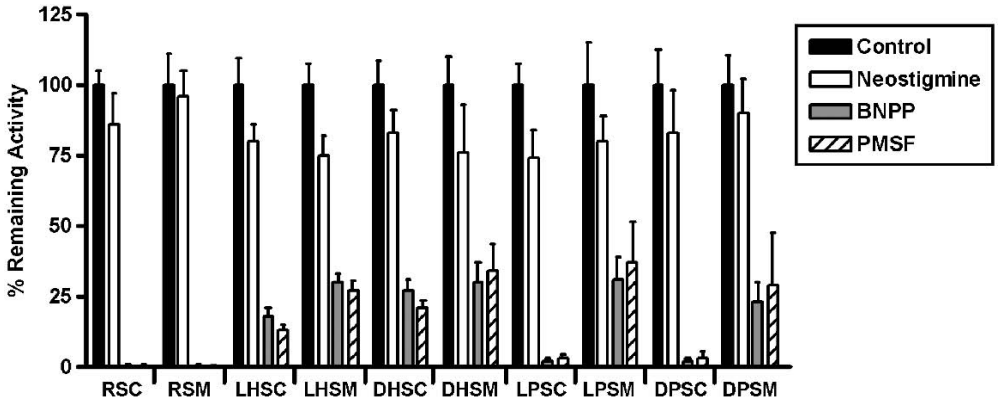

Fig. 3. Skin hydrolysis reaction phenotyping with esterase inhibitors. Subcellular skin fractions were preincubated with vehicle control, neostigmine (1 μM), *bis*-(*para*-nitrophenyl) phosphate (1 mM), or phenylmethylsulfonyl fluoride (1 mM) for 15 min at 37°C. Hydrolysis reactions with NAc (100 μM) as substrate were carried out as described in Materials and Methods. The various enzyme samples tested were rat skin cytosol (RSC), rat skin microsomes (RSM), light human skin cytosol (LHSC), light human skin microsomes (LHSM), dark human skin cytosol (DHSC), dark human skin microsomes (DHSM), light minipig skin cytosol (LPSC), light minipig skin microsomes (LPSM), dark minipig skin cytosol (DPSC), and dark minipig skin microsomes (DPSM). The columns and error bars represent the mean and standard deviation, respectively, and represent three independent experiments performed in triplicate.

labile groups (i.e., soft drugs) that are stable in the skin long enough to act on their pharmacological targets and then would be inactivated shortly after entering the systemic circulation. Therefore, metabolism within the epidermis and plasma would reduce the systemic exposure of these compounds. The high levels of esterase activity in skin and plasma make esters an attractive option for designing topically applied soft drugs and prodrugs.

Models of topical skin transport exist, but there is little evidence that these models are suitable for drug metabolism as well. Therefore, we have undertaken the characterization of xenobiotic ester-metabolizing enzymes in the skin homogenates of rats, minipigs, and humans. We have chosen PNPA as a prototypical esterase substrate because it is a well-known substrate for all mammalian carboxylesterases (20). The ester NAc was also studied because it is less susceptible to nonenzymatic hydrolysis than PNPA (15). Numerous esterases have been identified in mammalian tissues, which may explain in part the different values for maximal velocities (V_{max}) and apparent affinities (K_m) between laboratories. Nevertheless, many of our kinetic parameters agreed with previously reported values in the literature (see above) and with results of collaborators from other laboratories (data not shown).

Substrate-dependent inhibition by NAc was observed in minipig cytosol and in fractions of liver from all species. Substrate inhibition has been previously described for acetylcholinesterase, an enzyme present in skin. A peripheral binding site for acetylcholine has been identified by inhibition studies and through crystallography experiments (21,22). The K_s of acetylcholine for the secondary binding site was approximately 1 mM, a value similar to the K_i values determined for NAc in the present studies (Tables II and VI). Others have postulated that substrate binding to the peripheral site may block dissociation of product and therefore may slow the turnover of substrate. Additionally, allosteric activation has been observed for carboxylesterases and acetylcholinesterase (23). It is possible that the differences between minipig skin and the other species are derived from varying expression levels of NAc-inhibited esterases. Further experiments will be needed to identify the esterases that exhibit substrate-dependent inhibition by NAc and to compare substrate selectivity of minipig and human skin carboxylesterase activity.

Selective inhibitors have been commonly used to differentiate esterase isoforms within a particular tissue. Specific esterase inhibition allowed us to evaluate the different classes of esterases and their contributions to the hydrolysis rates observed in our kinetic experiments. We used neostigmine and BNPP as inhibitors of acetylcholinesterase and carboxylesterase, respectively. Hydrolysis activity in rat skin was derived almost entirely from carboxylesterase, with very little involvement by acetylcholinesterase. Human and minipig skin fractions were more sensitive to neostigmine and less sensitive to BNPP compared to rat skin. Acetylcholinesterases were more prominent in human and minipig skin, but carboxylesterases were the enzymes responsible for a majority of the substrate hydrolysis in these studies. The inhibitory profiles reemphasize the similarities between minipig and human skin.

Although grossly different in appearance, rat skin is often used as a model for human skin. However, large differences (orders of magnitude) were observed between rat and human skin esterase activity. In these experiments, rat skin fractions displayed significantly higher esterase activity than either human or minipig skin. Therefore, rat skin may not be an appropriate model of human skin ester hydrolysis. In the present study, minipig skin was a better representative of human skin esterase activity than rat skin. The results presented here support the use of minipigs over rats as preclinical models of biotransformation in skin. Our evaluation of the three species of skin subcellular fractions suggests that skin from minipigs can be used to predict nonspecific esterase activity toward topically applied compounds in human skin.

ACKNOWLEDGMENTS

We thank Christopher Jewell and Faith M. Williams for helpful discussions and insights. We also thank Ann Payne for experimental contributions and careful examination of the manuscript.

REFERENCES

1. P. Ettmayer, G. L. Amidon, B. Clement, and B. Testa. Lessons learned from marketed and investigational prodrugs. *J. Med. Chem.* **47**:2393–2404 (2004).
2. M. K. Danks, C. L. Morton, C. A. Pawlik, and P. M. Potter. Overexpression of a rabbit liver carboxylesterase sensitizes human tumor cells to CPT-11. *Cancer Res.* **58**:20–22 (1998).
3. P. D. Senter, H. Marquardt, B. A. Thomas, B. D. Hammock, I. S. Frank, and H. P. Svensson. The role of rat serum carboxylesterase in the activation of paclitaxel and camptothecin prodrugs. *Cancer Res.* **56**:1471–1474 (1996).
4. K. B. Sloan. *Prodrugs: Topical and Ocular Drug Delivery*, Marcel Dekker, New York, 1992.
5. P. Soucek, R. Zuber, E. Anzenbacherova, P. Anzenbacher, and F. P. Guengerich. Minipig cytochrome P450 3A, 2A and 2C enzymes have similar properties to human analogs. *BMC Pharmacol.* **1**:11 (2001).
6. A. V. Gore, A. C. Liang, and Y. W. Chien. Comparative biomembrane permeation of tacrine using Yucatan minipigs and domestic pigs as the animal model. *J. Pharm. Sci.* **87**:441–447 (1998).
7. J. Baranova, E. Anzenbacherova, P. Anzenbacher, and P. Soucek. Minipig cytochrome P450 2E1: comparison with human enzyme. *Drug Metab. Dispos.* **33**:862–865 (2005).
8. C. Lobemeier, C. Tschoetschel, S. Westie, and E. Heymann. Hydrolysis of parabenes by extracts from differing layers of human skin. *Biol. Chem.* **377**:647–651 (1996).
9. W. Junge, K. Leybold, and B. Philipp. Identification of a nonspecific carboxylesterase in human pancreas using vinyl 8-phenyloctanoate as a substrate. *Clin. Chim. Acta* **94**:109–114 (1979).
10. A. Galli, P. Malmberg Aiello, G. Renzi, and A. Bartolini. *In-vitro* and *in-vivo* protection of acetylcholinesterase by eseroline against inactivation by diisopropyl fluorophosphate and carbamates. *J. Pharm. Pharmacol.* **37**:42–48 (1985).
11. S. H. Sterri, B. A. Johnsen, and F. Fonnum. A radiochemical assay method for carboxylesterase, and comparison of enzyme activity towards the substrates methyl [1–14C] butyrate and 4-nitrophenyl butyrate. *Biochem. Pharmacol.* **34**:2779–2785 (1985).
12. Y. Yoshigae, T. Imai, M. Taketani, and M. Otagiri. Characterization of esterases involved in the stereoselective hydrolysis of ester-type prodrugs of propranolol in rat liver and plasma. *Chirality* **11**:10–13 (1999).
13. E. Heymann, W. Hoppe, A. Krusselmann, and C. Tschoetschel. Organophosphate sensitive and insensitive carboxylesterases in human skin. *Chem. Biol. Interact.* **87**:217–226 (1993).

14. B. Li, M. Sedlacek, I. Manoharan, R. Boopathy, E. G. Duysen, P. Masson, and O. Lockridge. Butyrylcholinesterase, paraoxonase, and albumin esterase, but not carboxylesterase, are present in human plasma. *Biochem. Pharmacol.* **70**:1673–1684 (2005).
15. W. Junge and K. Krisch. The carboxylesterases/amidases of mammalian liver and their possible significance. *CRC Crit. Rev. Toxicol.* **3**:371–435 (1975).
16. M. Kunert and E. Heymann. The equivalent weight of pig liver carboxylesterase (EC 3.1.1.1) and the esterase content of microsomes. *FEBS Lett.* **49**:292–296 (1975).
17. T. Satoh and M. Hosokawa. The mammalian carboxylesterases: from molecules to functions. *Annu. Rev. Pharmacol. Toxicol.* **38**:257–288 (1998).
18. E. Heymann and R. Mentlein. Carboxylesterases–amidases. *Methods Enzymol.* **77**:333–344 (1981).
19. M. Rooseboom, J. N. Commandeur, and N. P. Vermeulen. Enzyme-catalyzed activation of anticancer prodrugs. *Pharmacol. Rev.* **56**:53–102 (2004).
20. C. E. Wheelock, T. F. Severson, and B. D. Hammock. Synthesis of new carboxylesterase inhibitors and evaluation of potency and water solubility. *Chem. Res. Toxicol.* **14**:1563–1572 (2001).
21. T. Szegletes, W. D. Mallender, P. J. Thomas, and T. L. Rosenberry. Substrate binding to the peripheral site of acetylcholinesterase initiates enzymatic catalysis. Substrate inhibition arises as a secondary effect. *Biochemistry* **38**:122–133 (1999).
22. J. L. Sussman, M. Harel, F. Frolow, C. Oefner, A. Goldman, L. Toker, and I. Silman. Atomic structure of acetylcholinesterase from *Torpedo californica*: a prototypic acetylcholine-binding protein. *Science* **253**:872–879 (1991).
23. A. R. Main. Kinetic and structural relationships of transition monomeric and oligomeric carboxyl- and choline-esterases. *J. Environ. Sci. Health B* **18**:29–63 (1983).